Supporting information

Fluorine-donating electrolytes enable highly reversible 5 V Li metal batteries

Liumin Suo[1,2], Weijiang Xue[2], Mallory Gobet[3], Steve G. Greenbaum[3], Chao Wang[2], Yuming Chen[2], Wan-Lu Yang[4], Yang-Xing Li[4*] and Ju Li[2*]

[1] Key Laboratory for Renewable Energy, Beijing Key Laboratory for New Energy Materials and Devices, Beijing National Laboratory for Condensed Matter Physics, Institute of Physics, Chinese Academy of Sciences, School of Physical Sciences, University of Chinese Academy of Sciences, Beijing 100190, China

[2] Department of Nuclear Science and Engineering and Department of Materials Science and Engineering, Massachusetts Institute of Technology, Cambridge, MA 02139, USA.

[3] Department of Physics and Astronomy, Hunter College of CUNY, 695 Park Avenue, New York, NY 10065, USA.

[4] Watt Laboratory, Central Research Institute, Huawei Technologies Co., LTD., Bantian, Longgang District, Shenzhen 518129, China.

Materials. Lithium bis(trifluoromethane sulfonyl) imide ($LiN(SO_2CF_3)_2$, LiTFSI) (>98%), LiFSI, $LiClO_4$ and FEC were purchased from Tokyo Chemical Industry, Oakwood Products, Inc. and Sigma-Aldrich and Alfa respectively. All solvents (FEC and PC) were purified by the 4Å molecular sieve before used. The electrolytes are prepared by mol-salt in liter-solvent), which were coded by abbreviated concentrations Lithium bis(trifluoromethane sulfonyl) imide ($LiN(SO_2CF_3)_2$, LiTFSI) (>98%), LiFSI, $LiClO_4$ and FEC were purchased from Tokyo Chemical Industry, Oakwood Products, Inc. and Sigma-Aldrich and Alfa respectively. All solvents (FEC and PC) were purified by the 4Å molecular sieve before used.

Characterizations. Scanning electron microscopy (SEM) image was taken by Zeiss Merlin High-resolution Scanning electron microscope operating at 5 kV. X-ray photoelectron spectroscopy (XPS, aka ESCA) analysis was performed on Kratos AXIS with high depth resolution (10 nm or less), good elemental sensitivity (0.1 to 0.01 atomic percent), and lateral resolution down to 10 μm. Ar^+ etching was conducted at an argon partial pressure of $<10^{-8}$ Torr. All the samples were recovered from 2032 coin cell configuration after electrochemical cycling. The samples were washed by DME three times and then dried under vacuum for two hours before XPS measurement. A portable transfer vessel was used to process samples in glove-box and loaded into the XPS without exposure to air. The NMR diffusion experiments were done with a 400 SB Bruker AVANCE III spectrometer (9.4 T). Self-diffusion coefficients of FEC and FSI^- (^{19}F NMR), and Li^+ (^7Li NMR) were measured at 25°C using a stimulated echo sequence with bipolar pulses . Gradient strength was arrayed (16 values, linear increase,

g = 0-45 G/cm) for each experiment. Gradient pulse duration was δ/2 = 1.1-4 ms and diffusion delay was Δ = 200-750 ms.

Electrochemical Measurements. The ionic conductivity was measured with electrochemical impedance spectroscopy (EIS) using Gamry Reference 3000 over a temperature range of 10 to 50 °C. The samples were equilibrated in a thermostated water-bath, and at each set temperature the sample was left standing for at least 1 h before EIS were collected. The conductivity cell constants were pre-determined using 0.01M aqueous KCl standard solution at 25 °C. Linear sweep voltammetry (LSV) was applied to determinate the electrochemical stability window at a scanning rate of 10 mV/s using Al mesh as working electrode and Li strip as the counter and the reference electrode, which was carried out using Gamry electrochemical work station. Al mesh were thoroughly cleaned ultrasonically in high purity alcohol, and then washed three times with high purity water and dried before measurement. The diameter of cathode electrode is 10 mm. The Li anode electrodes used in half and full cell are thick Li chip (MTI Corporation) and thin pre-deposited Li on Cu foil (ϕ = 12 mm), respectively. Pre-deposited Li anode was obtained at a constant current of 0.05 mA for 40 hours. The cell was assembled in CR2032-type coin cell using 5 V Spinel $LiNi_{0.5}Mn_{1.5}O_4$ cathode, Li metal anode and glass fiber as separator. The cells were cycled galvanostatically on a Land BT2000 battery test system at room temperature.

The definition of Coulombic efficiency (CE). The CE values are defined with the following "clean-slate" procedure: one first pulls out all the Li^+ one can pull out in a copper-backed anode, making sure there is no cyclable Li reserve (although SEI, which contains non-cyclable Li, can exist physically) on the anode side. One then electrochemically deposit Q_{re} fresh Li^+ to the anode with $U_{max} \rightarrow U_{min}$, in the form of metallic lithium with varying degree of porosity. Lastly, one pulls Q_{ox} Li^+ out of the anode with $U_{min} \rightarrow U_{max}$, and compute $CE \equiv Q_{ox}/Q_{re}$.

Electrochemical impedance spectra (EIS) of LMA in HFF electrolyte. The data was collected in symmetric Li/Li cell in intervals of ten hours to characterize the growth of SEI. Fig. S7*B* shows that the charge-transfer resistance semi-circle increased from 50 Ω to 160 Ω with the resting time, indicated continuous SEI growth on lithium metal anode. The increase is asymptotic, so the growth rate of SEI was very fast in the initial stage and then gradually tapered off at the range of 150 ~160 Ω after 80 hours.

The definition of Donatable Fluorine Concentration (DFC). Donatable Fluorine Concentration (DFC) is defined straightforwardly as the molar sum of donatable F of salt and solvent molecules in 1-liter electrolyte solution. Considering that our electrolyte preparation by the ratio of salt to solvent with molar (salt) to liter (solvent) and the volume change before and after the mixture, we measured the densities of electrolytes listed in Table S5. Take 1 m LiFSI-FEC for example, the weight ratio of LiFSI to FEC is 187.07 to 1410 (density of FEC: 1.41 g/cc) which are correspond to the weight percentage of

11.7 % and 88.3 % respectively. Thus, 1.51 g/cc should have 0.9455 mmol LiFSI and 12.57 mmol FEC with F contribution number of 2 (LiFSI) and 1 (FEC). Finally, DFC of 1 m LiFSI-FEC is equal to 14.46 (0.9455*2 + 12.57).

The measurement of Ion transference number in LiFSI-FEC system. Ion transference number is the fraction of the total current carried in an electrolyte by a given ion. The cation transference number (t^+) and anion transference number (t^-), corresponding to the fraction of current carried out by the lithium ions and FSI^- ions respectively, were calculated by using following equations.

$$t^+ = \frac{D_{\mathrm{Li}^+}}{D_{\mathrm{Li}^+} + D_{\mathrm{TFSI}^-}} \qquad (1)$$

$$t^- = \frac{D_{\mathrm{TFSI}^-}}{D_{\mathrm{Li}^+} + D_{\mathrm{TFSI}^-}} \qquad (2)$$

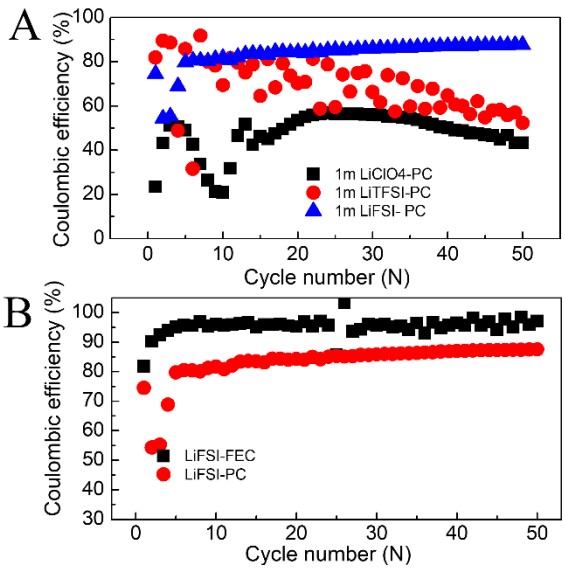

Fig. S1. The Coulombic efficiency of Li metal anode **(a)** in fluoride based salts (1m LiTFSI and LiFSI) and non-fluoride salt (1 m $LiClO_4$) dissolved in PC solvent, **(b)** in fluorinated (FEC) and non-fluorinated solvent (PC) contained 1 m LiFSI.

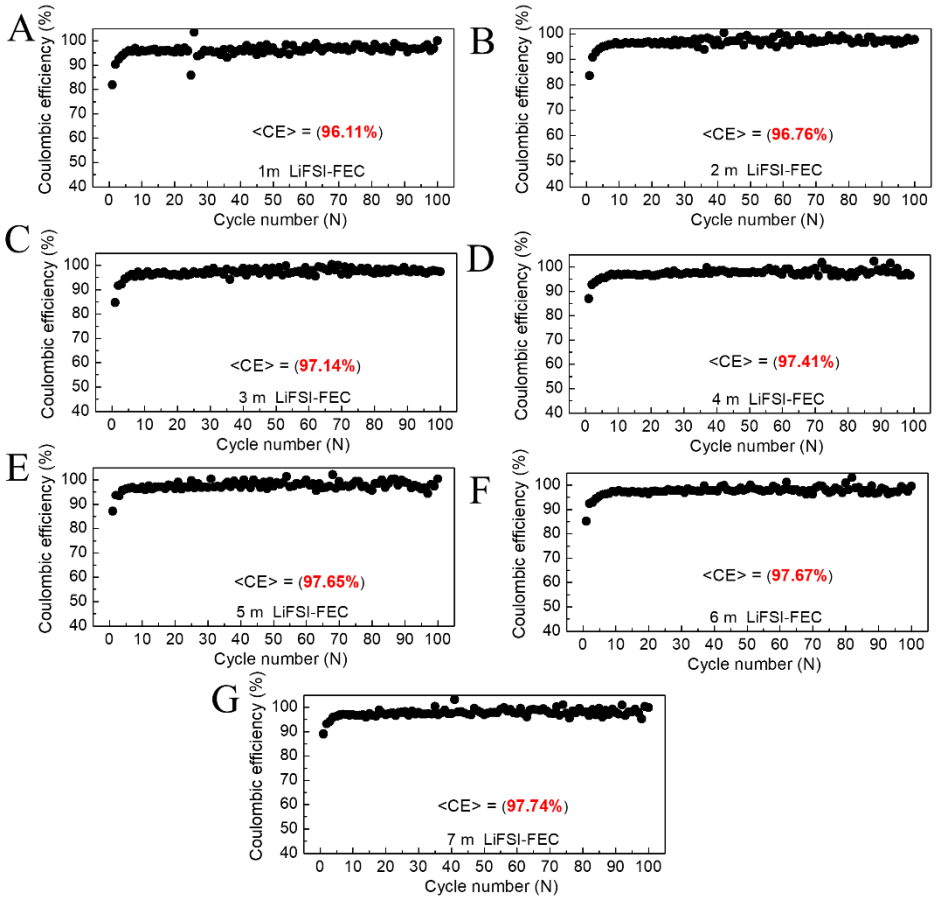

Fig. S2. Coulombic efficiencies (CE) of Li metal anode in different concentrated LiFSI in FEC and its average Coulombic efficiencies <CE> in the first 100 cycles, which is corresponding to Figure 1a and Figure 1c. (a) 1 m, (b) 2 m, (c) 3 m, (d) 4 m, (e) 5 m, (f) 6 m and (g) 7 m.

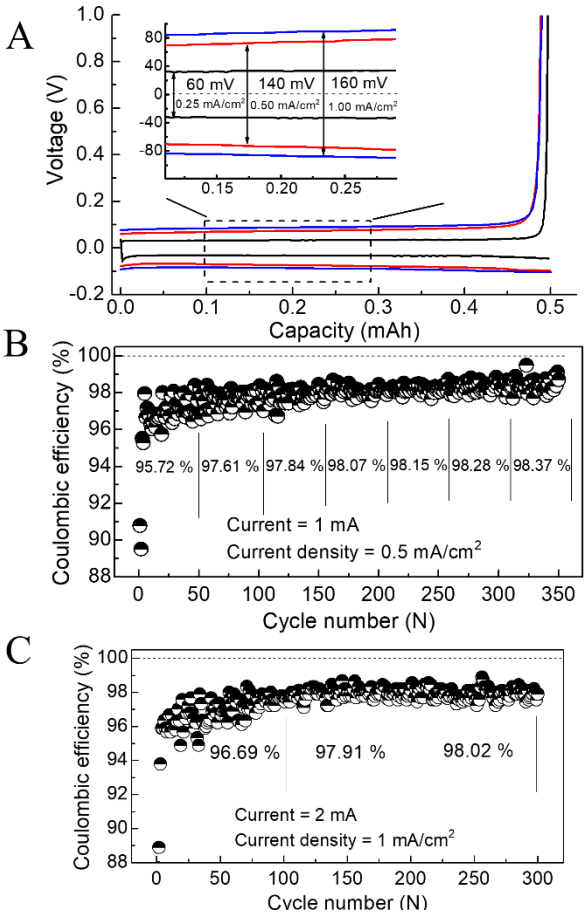

Fig. S3. The reversibility of Li metal anode in High Concentrated Full Fluoride-based (HFF) electrolytes (7 m LiFSI in FEC). (*A*) The initial Li deposition-dissolution profiles on Cu foil at different current density (0.25 mA/cm^2, 0.50 mA/cm^2 and 1.00 mA/cm^2), (*B*) and (*C*) the cycle Coulombic efficiencies of Li anode at 0.50 mA/cm^2 and 1.00 mA/cm^2.

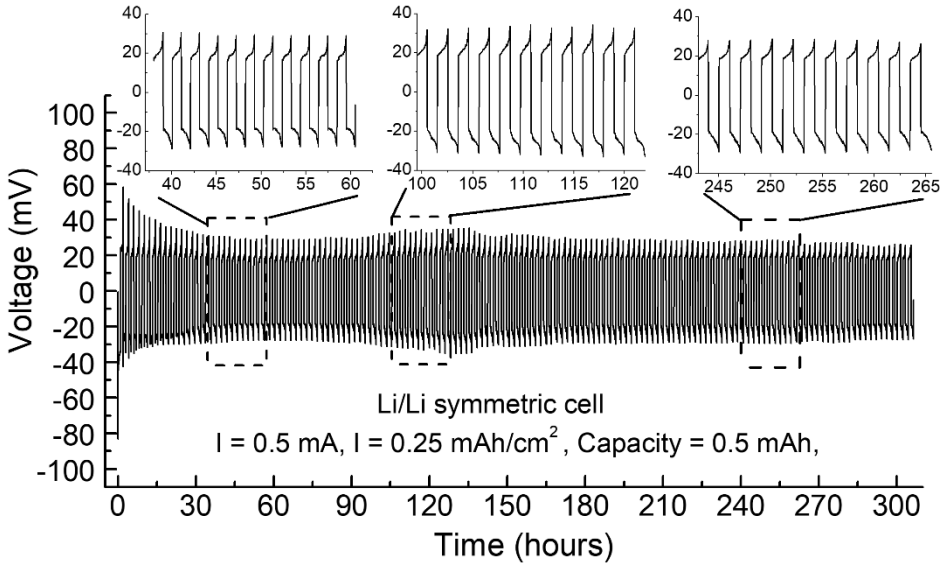

Fig. S4. The reversibility of Li metal anode in Symmetric Li/Li cell with HCFF electrolyte (7 m LiFSI in

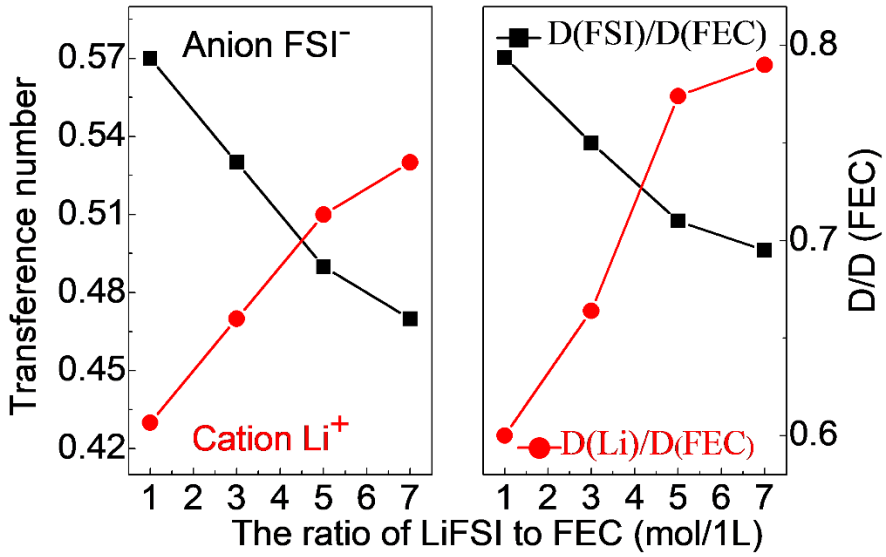

Fig. S5. Full Fluoride-based (HFF) electrolytes (LiFSI-FEC). Cation (Li ion) and anion (FSI^-) transference numbers and the self-diffusion coefficient ratio of Li^+/FSI^- to FEC at 25 °C.

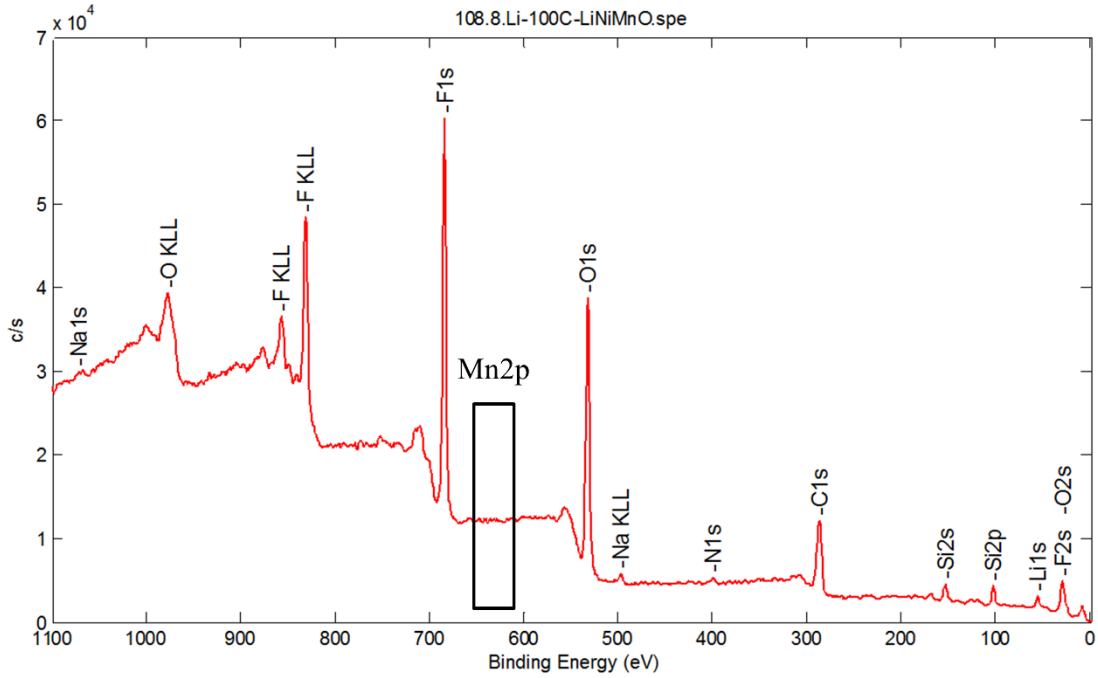

Fig. S6. XPS spectrum of Lithium anode after 100 cycles in half cell (LiNiMnO4/HFF/Li)

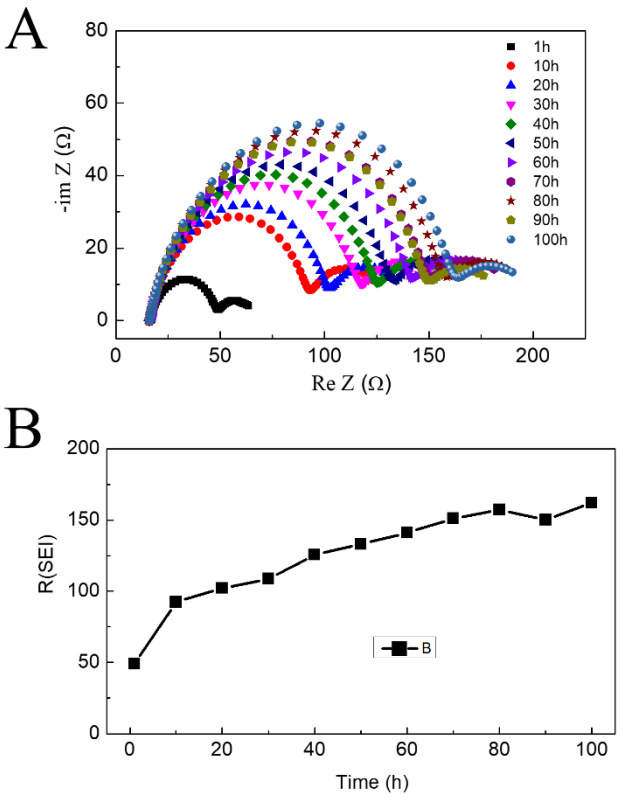

Fig. S7. The impedance of symmetric Li/Li cell with the resting time. (*A*) The impedance spectra of symmetric Li/Li cell in FF electrolyte at different rest times and (*B*) The change of SEI resistance with the increasing of resting time.

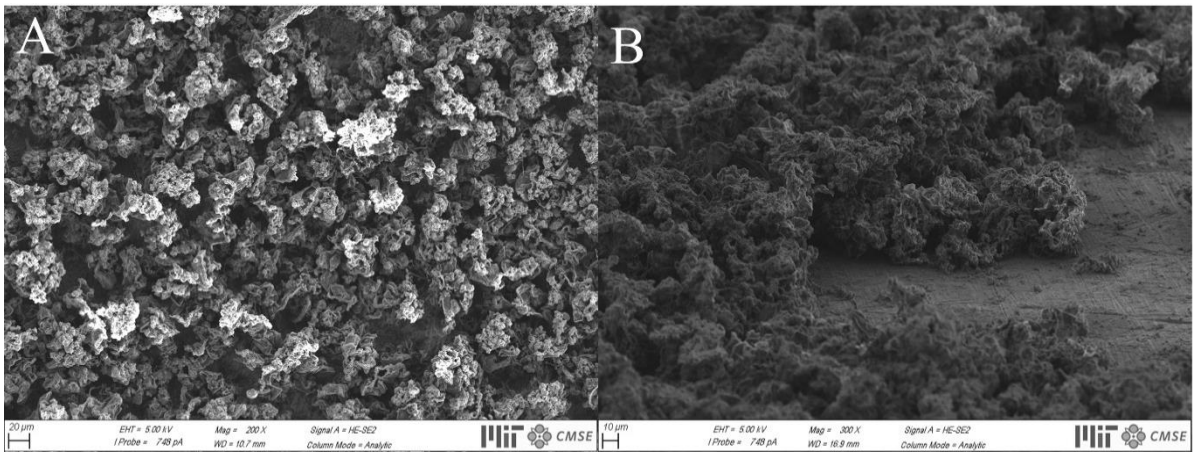

Fig. S8. The morphology of Li deposition on Cu foil. (*A*) Low magnification SEI image, (*B*) The cross-section view of SEM image.

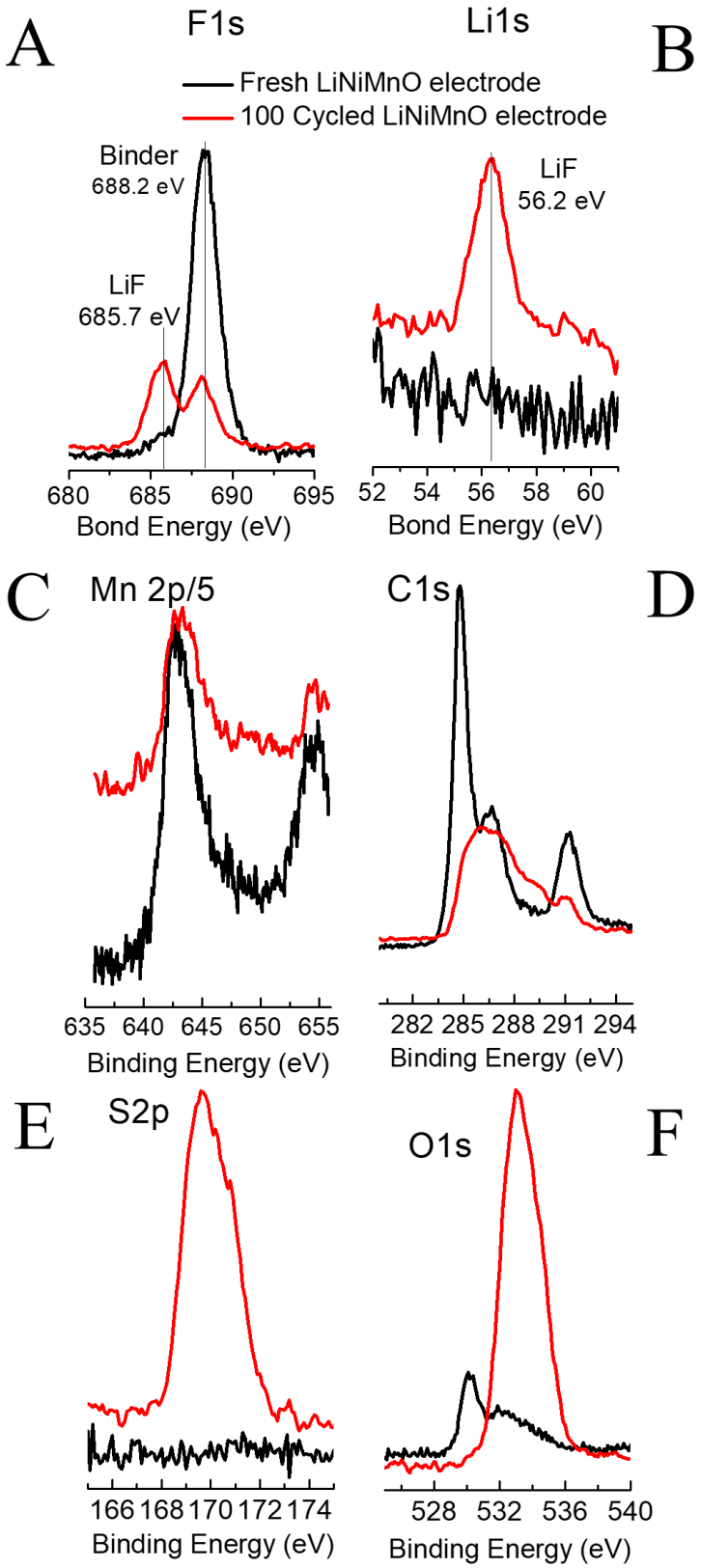

Fig. S9. XPS spectra of LiNMO electrode in HCFF electrolyte before and after 100 cycles. (*A*) F_{1s} and (*B*) Li_{1s}, (*C*) Manganese element, Mn 2p/5, (*D*) Carbon element, C1s, (*E*) Sulfur element, S2p and (*F*) Oxygen element, O1

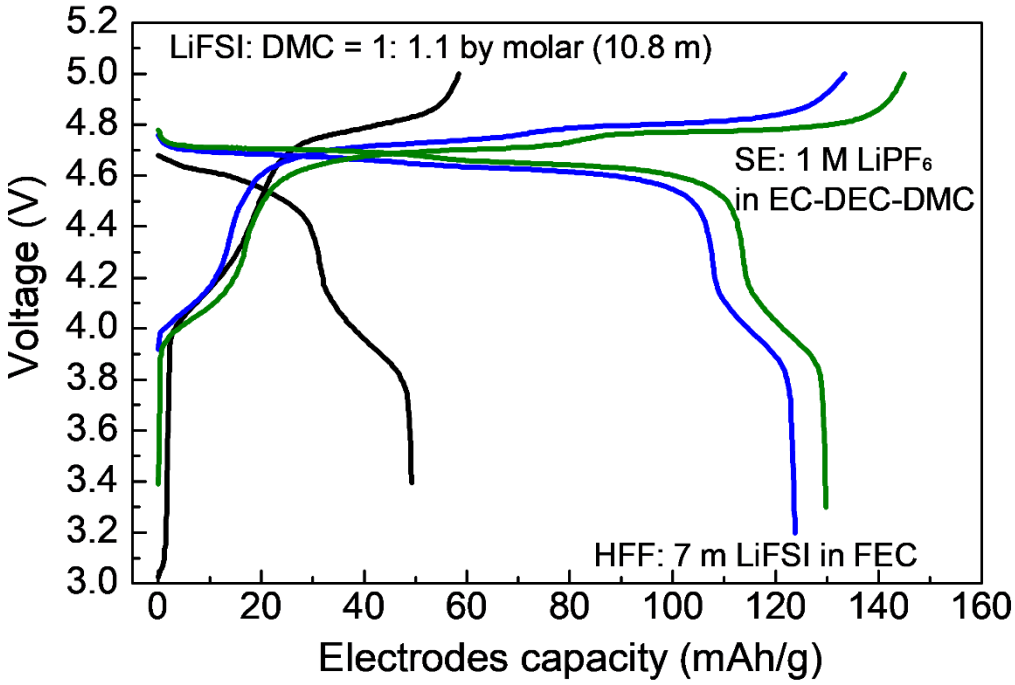

Fig. S10. The galvanostatic charge-discharge profiles of $LiNi_{0.5}Mn_{1.5}O_4$/HCFF electrolyte, LiFSI:DMC=1.1.1 by molar and SE/Li system in half cell, where the Li mole ratio of cathode to anode is above 1:100.

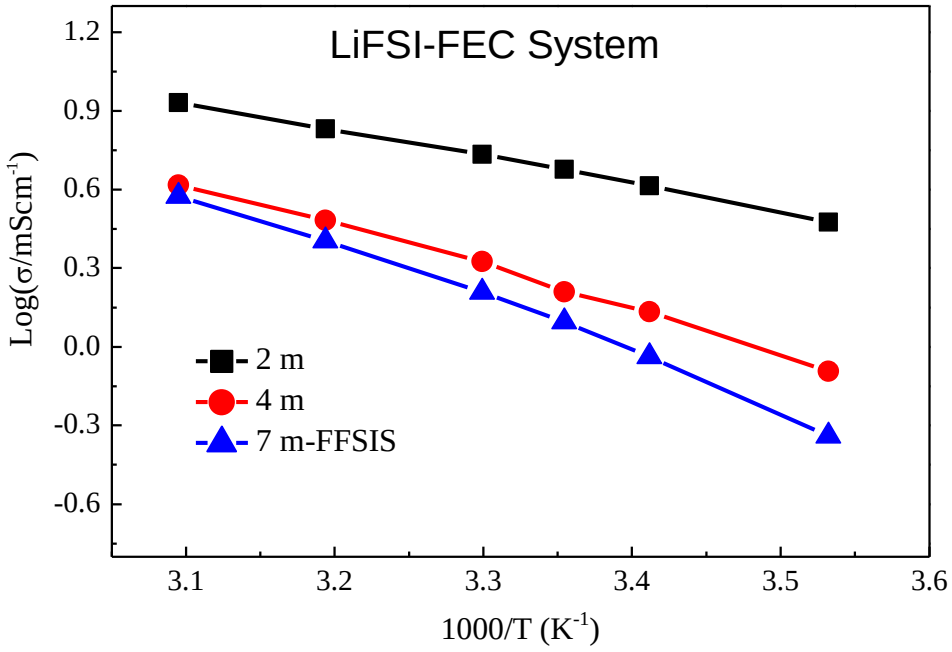

Fig. S11. Arrhenius plots of Lithium ion conductivity (σ) of LiFSI-FEC system in temperature range of 10 ºC ~ 50 ºC.

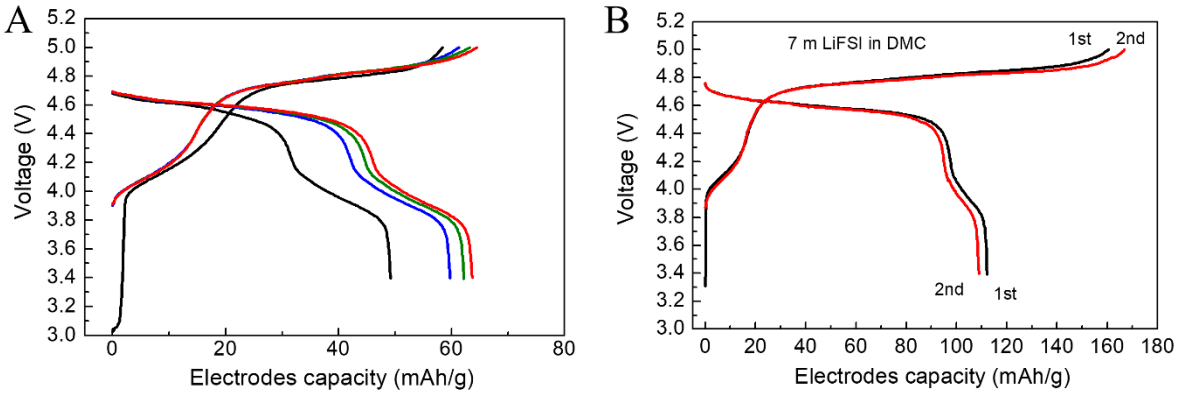

Fig. S12. The galvanostatic charge-discharge profiles of $LiNi_{0.5}Mn_{1.5}O_4$/ Li system in half cell, where the Li mole ratio of cathode to anode is above 1:100. (*A*) HFC：LiFSI : DMC = 1:1.1 by molar ratio, (*B*) 7 m LiFSI in DMC.

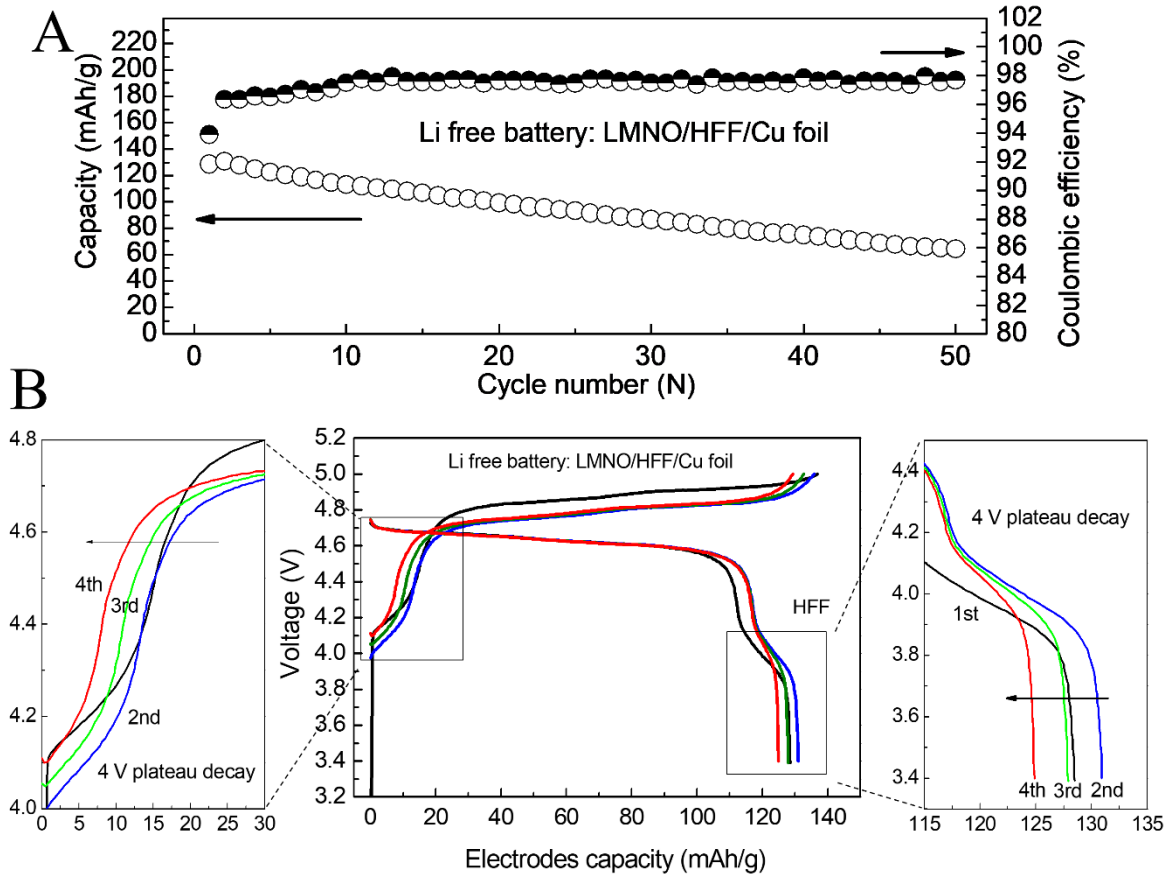

Fig. S13. The electrochemical performance of 5 V Li free battery constructed on LiNMO/HFF/Cu foil. (*A*) the cyclic life and columbic efficiency, (*B*) the charge-discharge initial profiles ($1^{st} \sim 4^{th}$).

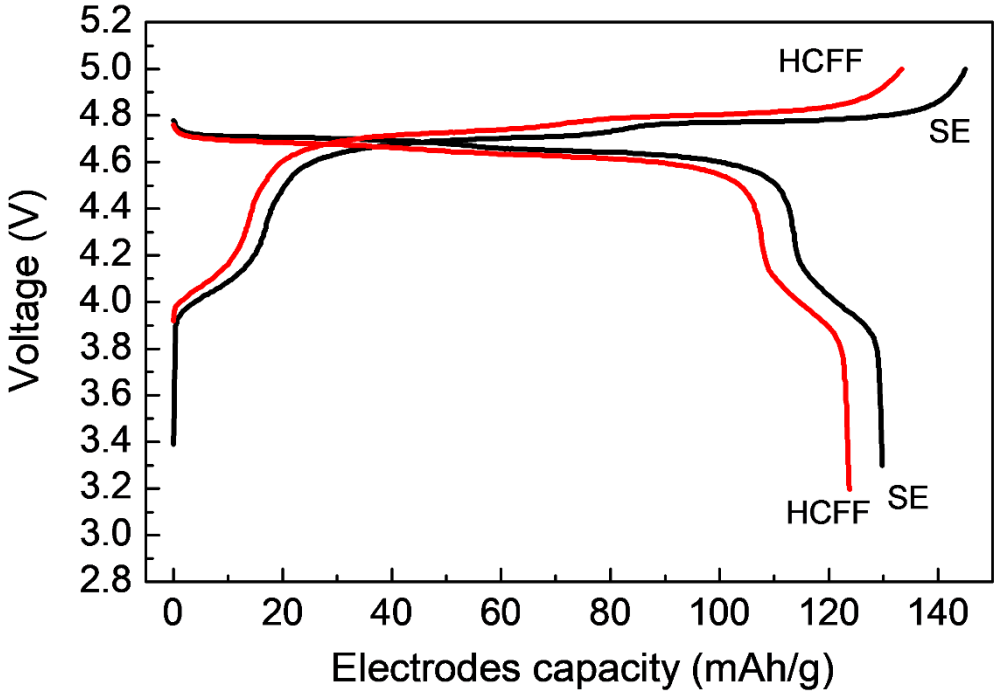

Fig. S14. Galvanostatic charge-discharge profiles of $LiNi_{0.5}Mn_{1.5}O_4$/HFF or SE /Li system in full cell

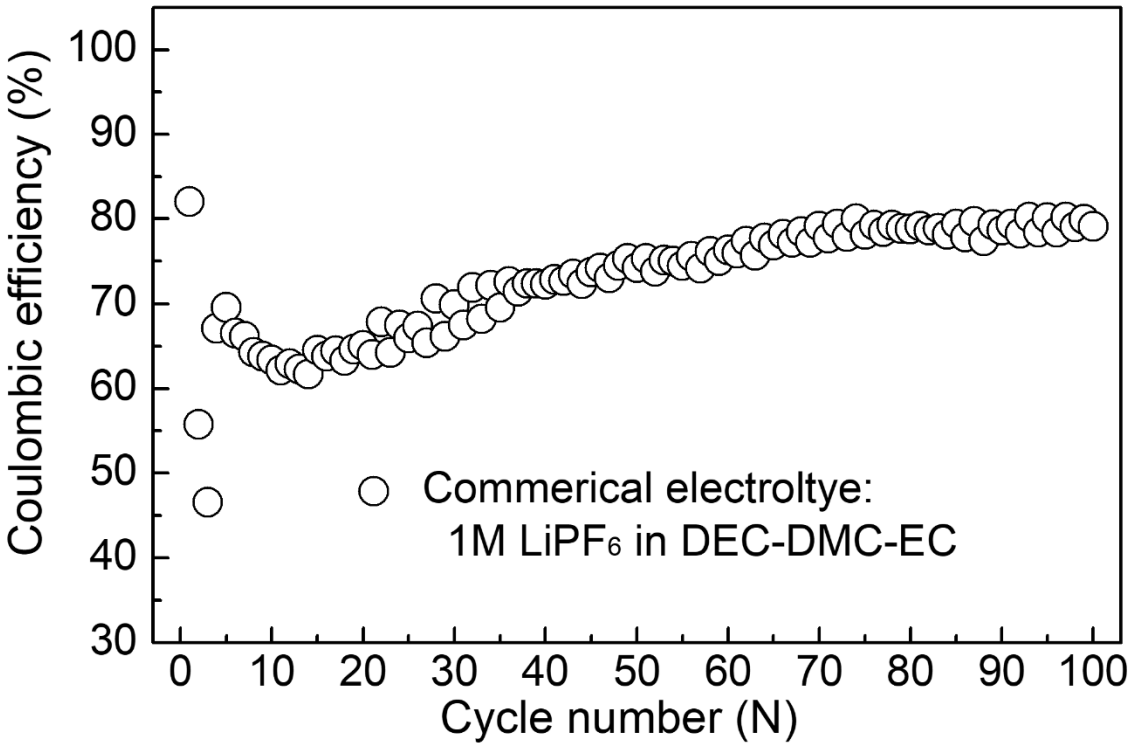

Fig. S15. The cycle coulombic efficiencies of Li anode in commercial electrolyte: 1M $LiPF_6$ in DEC-DMC-EC (BASF). The deposited/dissolved current density is 0.25 mA/cm^2 with the capacity of 0.5 mAh.

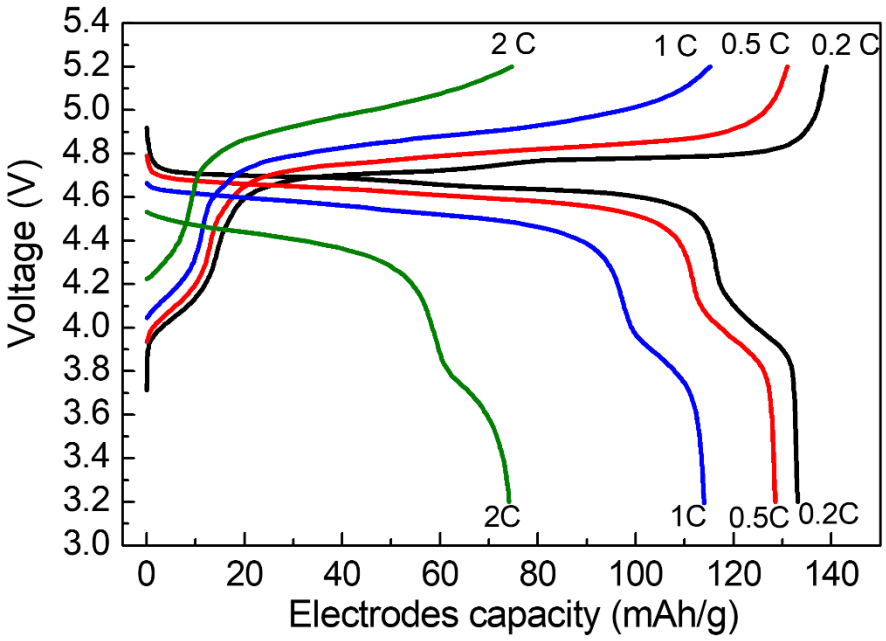

Fig. S16. The rate capability of full cell with HFF electrolyte. (*C*). The charge-discharge profile at different rates (0.2C, 0.5C, 1C and 2C), (*D*) the discharge capacity at the different rates.

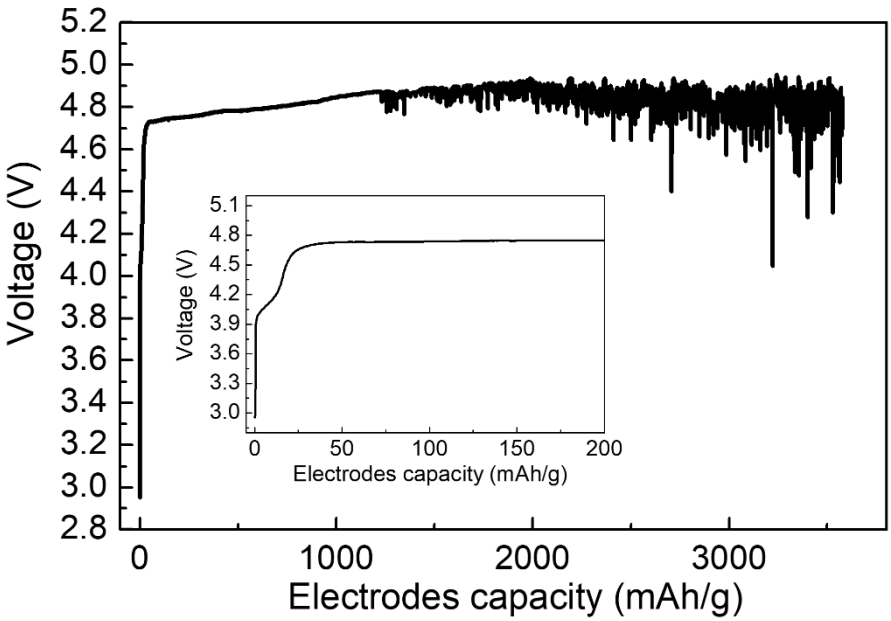

Fig. S17. The first charge profile of LiNMO/Li with 4M LiFSI in DME electrolyte

Table S1. The capacity and operating voltage of cathodes

Cathode	Voltage vs Li (V)	Theoretical capacity (mAh/g)	The real capacity
$LiFePO_4$	3.4	170	150
$LiCoO_2$	3.7	145	145
LiMn2O4	4.0	148	120
$LiNi_{0.5}Mn_{1.5}O_4$	4.7	146	130

Table S2. The capacity and operating voltage of graphite and Li metal anodes

Anode	Voltage vs Li (V)	Theoretical capacity (mAh/g)	The real capacity (mAh/g)
Graphite	0.1	375	360
Li metal	0	3860	3860

Table S3. The energy density calculation of graphite based Li ion batteries

Graphite based Li ion batteries	Output Voltage (V)	Theoretical capacity (mAh/g)	The real capacity (mAh/g)	Energy density (Wh/kg)
$LiFePO_4$/G	3.3	170/375	150 /360	349
$LiCoO_2$/G	3.6	145/375	145/360	373
$LiMn_2O_4$/G	3.9	148/375	120/360	351
$LiNi_{0.5}Mn_{1.5}O_4$/G	4.6	146/375	130/360	440

Table S4. The energy density calculation of Li-Free batteries

Li-Free batteries	Output Voltage (V)	Theoretical capacity (mAh/g)	The real capacity (mAh/g)	Energy density (Wh/kg)
$LiFePO_4$	3.4	170	150	510
$LiCoO_2$	3.7	145	145	536
$LiMn_2O_4$	4.0	148	120	480
$LiNi_{0.5}Mn_{1.5}O_4$	4.7	146	130	611

Table S5. DFC of different F donated electrolytes

Electrolyte	Salt (mol)	Solvent (Liter)	Density (g/cc)	DFC
1 m $LiClO_4$-PC	1 mol	1 L	1.24	0
1 m LiTFSI-PC	1 mol	1 L	1.27	0.851
1 m LiFSI-PC	1 mol	1 L	1.26	1.810
1 m LiFSI-FEC	1 mol	1 L	1.51	14.46
2 m LiFSI-FEC	2 mol	1 L	1.56	15.12
3 m LiFSI-FEC	3 mol	1 L	1.58	15.47
4 m LiFSI-FEC	4 mol	1 L	1.60	15.79
5 m LiFSI-FEC	5 mol	1 L	1.61	15.99
6 m LiFSI-FEC	6 mol	1 L	1.66	16.58
7 m LiFSI-FEC	7 mol	1 L	1.68	16.86

Table S6. NMR data for LiFSI-FEC electrolytes

Electrolyte mol/ 1L	Self-diffusion coefficient (in m^2/s) at 25°C			Li ion Transference Number	Anion Transference Number
LiFSI-FEC	D_{FEC}	D_{FSI^-}	D_{Li^+}	t_{Li}	t_{FSI}
1m	1.70E-10	1.35E-10	1.02E-10	0.43	0.57
3m	5.48E-11	4.11E-11	3.64E-11	0.47	0.53
5m	1.76E-11	1.25E-11	1.31E-11	0.51	0.49
7m	9.56E-12	6.65E-12	7.53E-12	0.53	0.47